Interaction Notes

Note 561

July 2000

Full-wave transmission-line theory (FWTLT) for the analysis of three-dimensional wire like structures

Heiko Haase and Jürgen Nitsch

Otto-von-Guericke-Universität Magdeburg
Institut für Grundlagen der Elektrotechnik und Elektromagnetische Verträglichkeit
Postfach 4120
39016 Magdeburg
Germany

Abstract

This paper presents a generalized transmission-line theory, which is useful to describe the wave propagation along as well as the field coupling to almost arbitrary three-dimensional wire structures. In contrast to the classical transmission-line theory this new theory is a full-wave description based on generalized telegraphers equations. Whereas the mathematical structure of these equations is preserved, the coefficients (the per unit length parameters) are redefined in order to represent the intrinsic behavior of the wire structure. Due to the full-wave description all EM – phenomena, e.g., radiation, are taken into account. Measurements as well as MoM simulations were performed to validate the predicted data.

1 Introduction

The Transmission-Line Theory (TLT), as a tool for the analysis and the design of the electrical interconnections between elements, components, and systems, plays an important role in electromagnetic compatibility. However, due to the limitation that only a quasi TEM mode is described in the classical theory, it is restricted to certain cases, where the connection structures can be regarded as parallel (althought they really do not have to be) and their cross sectional extent is much smaller than the considered wave length. This also includes the nonuniform transmission lines where the per unit length parameters become position dependent.

Otherwise full-wave techniques like the Method of Moments (MoM) or Partial Element Equivalent Circuit (PEEC) must be used to analyze given interconnection structures.

In this paper a new method is presented which circumvents this procedure for a huge class of interconnection structures. By now the new theory covers transmission-line like wire structures. This basically means transmission lines built of thin wires. The wires do not have to be in parallel, they can be bent, loops, however, are not allowed.

The method represents a generalized transmission-line theory and is based on Maxwell's equations. In contrast to the classical TLT it is a full-wave theory (Full Wave Transmission-Line Theory FWTLT) and therefore also includes radiation effects. However, the mathematical structure of the telegraphers equations is preserved, thus known techniques to solve these equations can be used. Also the results are well suited for the treatment of interconnections on PCBs and radiation losses at high frequencies of all wire structures.

Different from [8] no series development of the current is performed. The telegraphers equations are derived without any approximation (besides a reasonable thin wire approximation) from Maxwell's theory.

2 Basic equations for lossless three-dimensional wire structures

The electric field at an arbitrary point $\boldsymbol{r}$ in the vicinity of some scattering objects in a lossless, homogeneous, and isotropic medium can be expressed as the sum of an incident field $\boldsymbol{E}^{(i)}$ and the scattered field $\boldsymbol{E}^{(s)}$:

$$\boldsymbol{E}(\boldsymbol{r}) = \boldsymbol{E}^{(i)}(\boldsymbol{r}) + \boldsymbol{E}^{(s)}(\boldsymbol{r})\,. \tag{1}$$

The incident field is determined in the absence of the objects. The scattered field can be expressed by the electric (φ) and magnetic potential ($\boldsymbol{A}$), respectively:

$$\boldsymbol{E}^{(s)}(\boldsymbol{r}) = -\mathrm{grad}\varphi(\boldsymbol{r}) - j\omega\boldsymbol{A}(\boldsymbol{r})\,. \tag{2}$$

Here the potentials are calculated by the following expressions:

$$\varphi(\boldsymbol{r}) = \frac{1}{\varepsilon} \int G(\boldsymbol{r},\boldsymbol{r}')\,\varrho(\boldsymbol{r}')\,\mathrm{d}^3r', \tag{3}$$

$$\boldsymbol{A}(\boldsymbol{r}) = \mu \int G(\boldsymbol{r},\boldsymbol{r}')\,\boldsymbol{J}(\boldsymbol{r}')\,\mathrm{d}^3r', \tag{4}$$

where the free-space Green's function is given by:

$$G(\boldsymbol{r},\boldsymbol{r}') = \frac{\mathrm{e}^{-jk|\boldsymbol{r}-\boldsymbol{r}'|}}{4\pi|\boldsymbol{r}-\boldsymbol{r}'|}. \tag{5}$$

If the scattering objects are solely thin wires the **thin wire approximation** can be applied to (3) and (4). Along each wire the charge density ϱ becomes the charge per unit length q_i, while the current vector density $\boldsymbol{J}$ is represented by the current i_i, with the direction of the tangential unit vector $\boldsymbol{e}_{t_i}$. The index i denotes the number of the wire. The integration over the volume is reduced to line integrals along the length l_i of each individual wire. Every wire is described by a parametrized curve with the corresponding curve parameter s_i (see Fig. 1). Now, placing the

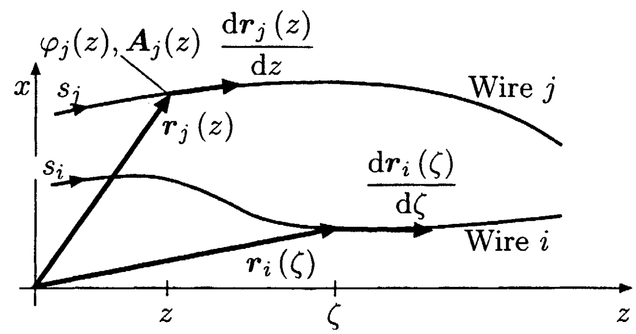

Figure 1: n-Wire Structure with the relevant variables.

observation point $\boldsymbol{r}$ directly onto one wire j the potentials read:

$$\varphi_j(s_j) = \frac{1}{\varepsilon} \sum_{i=1}^{n} \int_{l_i} q_i(s_i) \cdot G(\boldsymbol{r}_j(s_j), \boldsymbol{r}_i(s_i))\,\mathrm{d}s_i, \tag{6}$$

$$\boldsymbol{A}_j(s_j) = \mu \sum_{i=1}^{n} \int_{l_i} i_i(s_i) \cdot \boldsymbol{e}_{t_i}(s_i) \cdot G(\boldsymbol{r}_j(s_j), \boldsymbol{r}_i(s_i))\,\mathrm{d}s_i \tag{7}$$

where n indicates the total number of the wires. For further steps it is convenient to perform a transition from the local curve parameter s_i to a global coordinate, e.g. z. All position dependent quantities are then expressed as a function of this new variable. Further, the tangential unit vector is given by the derivative of the spatial vector $\boldsymbol{r}$ with respect to the curve parameter:

$$\boldsymbol{e}_{t_i} = \frac{\mathrm{d}\boldsymbol{r}_i}{\mathrm{d}s_i} = \frac{\mathrm{d}\boldsymbol{r}_i}{\mathrm{d}z}\frac{\mathrm{d}z}{\mathrm{d}s_i}. \tag{8}$$

If the wires are ideally conducting the tangential component of the electric field must vanish ($\boldsymbol{e}_t \cdot \boldsymbol{E} = 0$). Applying this boundary condition to (1) and inserting (7) into (2), and (2) into (1) yields:

$$\frac{\mathrm{d}\varphi_j(z)}{\mathrm{d}z} = -\,j\omega \sum_{i=1}^{n} \int_{z_0}^{z_l} i_i(\zeta)\, k_{ji}^{L}(z,\zeta)\ \mathrm{d}\zeta + v_j^{(i)}(z) \tag{9}$$

The integral kernel then turns out to be:

$$k_{ji}^{L}(z,\zeta) = \mu \frac{\mathrm{d}\boldsymbol{r}_j(z)}{\mathrm{d}z} \cdot \frac{\mathrm{d}\boldsymbol{r}_i(\zeta)}{\mathrm{d}\zeta} G(\boldsymbol{r}_j(z)\,, \boldsymbol{r}_i(\zeta)) \tag{10}$$

and the per unit length voltage, induced by the external field, reads

$$v_j^{(i)}(z) = \boldsymbol{e}_{t_j}(z) \cdot \boldsymbol{E}^{(i)}(\boldsymbol{r}_j(z))\,. \tag{11}$$

With the (thin wire) continuity equation $q_i = -\frac{1}{j\omega}\frac{\mathrm{d}i_i}{\mathrm{d}s_i}$ the electric potential (6) becomes

$$\varphi_j(z) = -\,\frac{1}{j\omega} \sum_{i=1}^{n} \int_{z_0}^{z_l} \frac{\mathrm{d}i_i(\zeta)}{\mathrm{d}\zeta} k_{ji}^{C}(z,\zeta)\ \mathrm{d}\zeta. \tag{12}$$

where the integral kernel k_{ij}^{C} is expressed by

$$k_{ji}^{C}(z,\zeta) = \frac{1}{\varepsilon} G(\boldsymbol{r}_j(z)\,, \boldsymbol{r}_i(\zeta)) \tag{13}$$

Equation (9) describes the inductive coupling of the wires. The Green's function in k_{ji}^{L} is multiplied by a dot product factor of the tangential vectors of the wires, which takes the vector character of the current density into account. In contrast to this, (12) describes the capacitive coupling. Since the charge density is a scalar variable, k_{ji}^{C} does only depend on the distance, but not on the direction of the wires. Only in the case that all wires are in parallel (like in the classical transmission-line theory) the dot product becomes one and both kernels are, besides a constant factor, equal.

Often it is necessary to consider wires, which are located above a perfectly conducting ground plane. This can be done by using the image theory where the ground plane is replaced by the corresponding wire images. The signs of all currents and potentials in the images are inverted. To accomplish this it is sufficient to replace the integral kernels with:

$$k_{ji}^{L}(z,\zeta) = \mu \left[\frac{\mathrm{d}\boldsymbol{r}_j(z)}{\mathrm{d}z} \cdot \frac{\mathrm{d}\boldsymbol{r}_i(\zeta)}{\mathrm{d}\zeta} G(\boldsymbol{r}_j(z)\,, \boldsymbol{r}_i(\zeta)) - \frac{\mathrm{d}\boldsymbol{r}_j(z)}{\mathrm{d}z} \cdot \boldsymbol{A} \cdot \frac{\mathrm{d}\boldsymbol{r}_i(\zeta)}{\mathrm{d}\zeta} G(\boldsymbol{r}_j(z)\,, \boldsymbol{A} \cdot \boldsymbol{r}_i(\zeta)) \right] \tag{14}$$

$$k_{ji}^{C}(z,\zeta) = \frac{1}{\varepsilon} \Big[G(\boldsymbol{r}_j(z)\,, \boldsymbol{r}_i(\zeta)) - G(\boldsymbol{r}_j(z)\,, \boldsymbol{A} \cdot \boldsymbol{r}_i(\zeta)) \Big]. \tag{15}$$

The matrix $\boldsymbol{A}$ is the "reflection matrix" and is given by the position of the ground plane. If, for instance the ground plane is located in the y-z plane of the coordinate system, $\boldsymbol{A}$ is given by:

$$\boldsymbol{A} = \begin{bmatrix} -1 & 0 & 0 \\ 0 & 1 & 0 \\ 0 & 0 & 1 \end{bmatrix} .$$

The identical structure of (9) and (12) allows to combine both expressions into one supermatrix equation:

$$\begin{bmatrix} \boldsymbol{\varphi}'(z) \\ \boldsymbol{\varphi}(z) \end{bmatrix} = \int_{z_0}^{z_l} \overline{\boldsymbol{W}} \cdot \overline{\boldsymbol{K}}(z,\zeta) \cdot \overline{\boldsymbol{W}}^{-1} \begin{bmatrix} \boldsymbol{i}'(\zeta) \\ \boldsymbol{i}(\zeta) \end{bmatrix} \mathrm{d}\zeta + \begin{bmatrix} \boldsymbol{v}^{(i)}(z) \\ \boldsymbol{0} \end{bmatrix} . \tag{16}$$

The supermatrices $\overline{\boldsymbol{K}}$ and $\overline{\boldsymbol{W}}$ are given by

$$\overline{\boldsymbol{K}}(z,\zeta) = \begin{bmatrix} \boldsymbol{0} & \boldsymbol{K}^L(z,\zeta) \\ \boldsymbol{K}^C(z,\zeta) & \boldsymbol{0} \end{bmatrix} , \tag{17}$$

$$\overline{\boldsymbol{W}} = \begin{bmatrix} -j\omega\boldsymbol{1} & \boldsymbol{0} \\ \boldsymbol{0} & \boldsymbol{1} \end{bmatrix} . \tag{18}$$

The column vectors $\boldsymbol{\varphi}$ and $\boldsymbol{i}$ are composed of the elements φ_i and i_i, respectively. The matrices $\boldsymbol{K}^C$ and $\boldsymbol{K}^L$ consist of the elements k^L_{ij} and k^C_{ij}. The prime denotes the derivative with respect to the spatial coordinate z or ζ, respectively.

Equation (16) now becomes the basis for the generalized telegraphers equations. As can be seen (16) already has some similarities with these equations. The unknown quantities are the current and the electric potential and both occur themself or as their first derivative with respect to the spatial coordinate. Further, the potential is regarded as the equivalence to the voltage as in the classical transmission-line theory.

3 Generalized telegraphers equations

3.1 Derivation

In order to formally transform (16) to the generalized telegraphers equations, a function $\overline{\boldsymbol{T}}(z,\zeta)$ is introduced which "transports" the current vector from position z to ζ.

$$\begin{bmatrix} \boldsymbol{i}'(\zeta) \\ \boldsymbol{i}(\zeta) \end{bmatrix} = \overline{\boldsymbol{W}} \cdot \overline{\boldsymbol{T}}(z,\zeta) \cdot \overline{\boldsymbol{W}}^{-1} \cdot \begin{bmatrix} \boldsymbol{i}'(z) \\ \boldsymbol{i}(z) \end{bmatrix} . \tag{19}$$

So far $\overline{\boldsymbol{T}}(z,\zeta)$ is unknown. However, as will be shown later it is related to the solution of the generalized telegraphers equations. Equation (16) becomes

$$\begin{bmatrix} \boldsymbol{\varphi}'(z) \\ \boldsymbol{\varphi}(z) \end{bmatrix} = \overline{\boldsymbol{W}} \cdot \overline{\boldsymbol{R}}(z) \cdot \overline{\boldsymbol{W}}^{-1} \cdot \begin{bmatrix} \boldsymbol{i}'(z) \\ \boldsymbol{i}(z) \end{bmatrix} + \begin{bmatrix} \boldsymbol{v}^{(i)}(z) \\ \boldsymbol{0} \end{bmatrix} \tag{20}$$

where $\overline{\boldsymbol{R}}$ is given by

$$\overline{\boldsymbol{R}}(z) = \int\limits_{z_0}^{z_l} \overline{\boldsymbol{K}}(z,\zeta) \cdot \overline{\boldsymbol{T}}(z,\zeta)\ \mathrm{d}\zeta. \tag{21}$$

Rearranging (20) yields the generalized telegraphers equations for lossless conductors

$$\boxed{\begin{bmatrix} \boldsymbol{\varphi}'(z) \\ \boldsymbol{i}'(z) \end{bmatrix} = -j\omega \overline{\boldsymbol{P}}(z) \begin{bmatrix} \boldsymbol{\varphi}(z) \\ \boldsymbol{i}(z) \end{bmatrix} + \begin{bmatrix} \boldsymbol{v}^{(i)}(z) \\ \boldsymbol{0} \end{bmatrix}} \tag{22}$$

where the coefficient supermatrix $\overline{\boldsymbol{P}}$ reads

$$\overline{\boldsymbol{P}} = \begin{bmatrix} \boldsymbol{R}_{11}\boldsymbol{R}_{21}^{-1} & \boldsymbol{R}_{12} - \boldsymbol{R}_{11}\boldsymbol{R}_{21}^{-1}\boldsymbol{R}_{22} \\ \boldsymbol{R}_{21}^{-1} & -\boldsymbol{R}_{21}^{-1}\boldsymbol{R}_{22} \end{bmatrix}. \tag{23}$$

The off-diagonal matrices can be identified as the inductance and capacitance per unit length matrices, while the diagonal matrices are correction terms that occur due to discontinuities like nonuniformities or terminations, and are responsible for the radiation effects. They vanish when infinitely long, uniform transmission lines or wire structures in the quasi static case are considered.

3.2 General solution

The general solution of the generalized telegraphers equations (22) (with position dependent parameters) is obtained via the **product integral** as shown in [4, 1]:

$$\begin{bmatrix} \boldsymbol{\varphi}(z) \\ \boldsymbol{i}(z) \end{bmatrix} = \prod_{z_0}^{z} \mathrm{e}^{-j\omega\overline{\boldsymbol{P}}(\xi)\,\mathrm{d}\xi} \begin{bmatrix} \boldsymbol{\varphi}(z_0) \\ \boldsymbol{i}(z_0) \end{bmatrix} + \int\limits_{z_0}^{z} \prod_{\xi}^{z} \mathrm{e}^{-j\omega\overline{\boldsymbol{P}}(\xi)\,\mathrm{d}\xi} \begin{bmatrix} \boldsymbol{v}^{(i)}(\xi) \\ \boldsymbol{0} \end{bmatrix} \mathrm{d}\xi \tag{24}$$

where the product integral can be expressed by the infinite series

$$\begin{aligned} \prod_{z_0}^{z} \mathrm{e}^{-j\omega\overline{\boldsymbol{P}}(\xi)\,\mathrm{d}\xi} = \overline{\boldsymbol{1}} &+ \int\limits_{z_0}^{z} -j\omega\overline{\boldsymbol{P}}(\xi)\ \mathrm{d}\xi \\ &+ \int\limits_{z_0}^{z} -j\omega\overline{\boldsymbol{P}}(\xi) \int\limits_{z_0}^{\xi} -j\omega\overline{\boldsymbol{P}}(\zeta)\ \mathrm{d}\zeta\,\mathrm{d}\xi \\ &+ \ldots \end{aligned} \tag{25}$$

The evaluation of this series is mathematically challenging and only a few, but important practical cases can be solved in closed form [2, 3]. Numerically the product integral can be calculated by dividing the interval $[z_0, z_l]$ into k segments and computing the product directly [5]:

$$\prod_{z_0}^{z} \mathrm{e}^{-j\omega\overline{\boldsymbol{P}}(\xi)\,\mathrm{d}\xi} \approx \prod_{i=0}^{k} \mathrm{e}^{-j\omega\overline{\boldsymbol{P}}(\xi_i)\Delta\xi} \tag{26}$$

3.3 Determination of the coefficient matrix

For the determination of the coefficients it is sufficient to consider only the homogeneous part of the equations. With the aid of (22), (24) can be rearranged to

$$\begin{bmatrix} \boldsymbol{i}'(\zeta) \\ \boldsymbol{i}(\zeta) \end{bmatrix} = \overline{\boldsymbol{W}} \cdot \overline{\boldsymbol{Q}}(\zeta) \cdot \prod_{z}^{\zeta} \mathrm{e}^{-j\omega \overline{\boldsymbol{P}}(\xi)\,\mathrm{d}\xi} \cdot \overline{\boldsymbol{Q}}(z)^{-1} \cdot \overline{\boldsymbol{W}}^{-1} \cdot \begin{bmatrix} \boldsymbol{i}'(z) \\ \boldsymbol{i}(z) \end{bmatrix}, \tag{27}$$

where $\overline{\boldsymbol{Q}}$ is given by

$$\overline{\boldsymbol{Q}}(z) = \begin{bmatrix} \boldsymbol{R}_{21}(z)^{-1} & -\boldsymbol{R}_{21}(z)^{-1}\overline{\boldsymbol{R}}_{22}(z) \\ \boldsymbol{0} & \boldsymbol{1} \end{bmatrix} \tag{28}$$

By inspection of (27) and (19) it can be seen that $\overline{\boldsymbol{T}}$ is given by:

$$\overline{\boldsymbol{T}}(z,\zeta) = \overline{\boldsymbol{Q}}(\zeta) \cdot \prod_{z}^{\zeta} \mathrm{e}^{-j\omega \overline{\boldsymbol{P}}(\xi)\,\mathrm{d}\xi} \cdot \overline{\boldsymbol{Q}}(z)^{-1} \tag{29}$$

Substituting (29) into (21) yields an integral equation for the determination of the parameter supermatrix $\overline{\boldsymbol{R}}$:

$$\overline{\boldsymbol{R}} = \int_{z_0}^{z_l} \overline{\boldsymbol{K}}(z,\zeta) \cdot \overline{\boldsymbol{Q}}(\zeta) \cdot \prod_{z}^{\zeta} \mathrm{e}^{-j\omega \overline{\boldsymbol{P}}(\xi)\,\mathrm{d}\xi} \cdot \overline{\boldsymbol{Q}}(z)^{-1}\,\mathrm{d}\zeta. \tag{30}$$

This equation can not be solved directly, however, an iterative procedure can be used to determine the parameters. The quasi static parameters, which can be easily obtained are used as starting values.

3.3.1 Quasi static parameters

In the quasi static case it is assumed that the wavelength is much larger than the extent of the whole wire structure. Thus, the exponential term in the Green's function becomes one ($\mathrm{e}^{-jk|\boldsymbol{r}(z)-\boldsymbol{r}(\zeta)|} \approx 1$, $\overline{\boldsymbol{K}}^{(0)} := \overline{\boldsymbol{K}}\,(w=0)$). Further, for the calculation of the line parameters the potential as well as the current along each wire is considered to be constant. Therefore, the product integral is the unity matrix:

$$\prod_{z}^{\zeta} \mathrm{e}^{-j\omega \overline{\boldsymbol{P}}(\xi)\,\mathrm{d}\xi} = \overline{\boldsymbol{1}}. \tag{31}$$

Moreover, doing a series expansion of $\overline{\boldsymbol{Q}}\,(\zeta)$ in the vicinity of z,

$$\overline{\boldsymbol{Q}}\,(\zeta) = \overline{\boldsymbol{Q}}\,(z) + \left.\frac{\mathrm{d}\overline{\boldsymbol{Q}}\,(\zeta)}{\mathrm{d}\zeta}\right|_{\zeta=z} (\zeta - z) + \ldots \tag{32}$$

and neglecting higher than first oder terms, gives a low frequency approximation for $\overline{\boldsymbol{R}}$:

$$\overline{\boldsymbol{R}}^{(0)}(z) = \int_{z_0}^{z_l} \overline{\boldsymbol{K}}^{(0)}(z,\zeta)\, \mathrm{d}\zeta. \tag{33}$$

Thus, the quasi static parameters of the generalized telegraphers equations are:

$$\overline{\boldsymbol{P}}^{(0)}(z) = \begin{bmatrix} \mathbf{0} & \boldsymbol{R}_{12}^{(0)}(z) \\ \boldsymbol{R}_{21}^{(0)}(z)^{-1} & \mathbf{0} \end{bmatrix} \tag{34}$$

It is interesting to note that, if (33) is applied to a uniform transmission line the classical transmission-line parameters , see e.g. [6, 7], are obtained.

3.3.2 Full-wave parameters

In order to determine a full-wave solution with the proposed theory, (22) must be solved with the exact parameters, which arise from the exact solution of (30). However, an explicit closed form solution of this equation turns out to be extremely difficult for general wire geometries. Therefore, an iterative procedure is used to get an approximation of the wanted parameters:

$$\overline{\boldsymbol{R}}^{(n+1)}(z) = \int_{z_0}^{z_l} \overline{\boldsymbol{K}}(z,\zeta)\cdot \overline{\boldsymbol{Q}}^{(n)}(\zeta)\cdot \prod_{z}^{\zeta} \mathrm{e}^{-j\omega \overline{\boldsymbol{P}}^{(n)}(\xi)\,\mathrm{d}\xi} \cdot \overline{\boldsymbol{Q}}^{(n)}(z)^{-1}\, \mathrm{d}\zeta. \tag{35}$$

where $\overline{\boldsymbol{P}}^{(n)}$ and $\overline{\boldsymbol{Q}}^{(n)}$ are given by:

$$\begin{aligned} \overline{\boldsymbol{P}}^{(n)} &= \begin{bmatrix} \boldsymbol{R}_{11}^{(n)} \boldsymbol{R}_{21}^{(n)^{-1}} & \boldsymbol{R}_{12}^{(n)} - \boldsymbol{R}_{11}^{(n)} \boldsymbol{R}_{21}^{(n)^{-1}} \boldsymbol{R}_{22}^{(n)} \\ \boldsymbol{R}_{21}^{(n)^{-1}} & -\boldsymbol{R}_{21}^{(n)^{-1}} \boldsymbol{R}_{22}^{(n)} \end{bmatrix} \\ \overline{\boldsymbol{Q}}^{(n)} &= \begin{bmatrix} \boldsymbol{R}_{21}^{(n)^{-1}} & -\boldsymbol{R}_{21}^{(n)^{-1}} \boldsymbol{R}_{22}^{(n)} \\ \mathbf{0} & \mathbf{1} \end{bmatrix} \end{aligned} \tag{36}$$

The quasi static parameters are good starting values. Thus, it is sufficient to perform only one iteration to get very accurate results for most cases.

3.4 Equivalent circuit representation

It is well known, that the telegraphers equations can be represented as an equivalent circuit for an infinitesimal segment. The same can be done for the generalized telegraphers equations (see Fig. 2). The additional coefficients in the main diagonal turn out to be a voltage and a current source, just like the external sources in the classical transmission-line theory. However, these sources are controlled by the current and voltage of the line itself instead of incident fields.

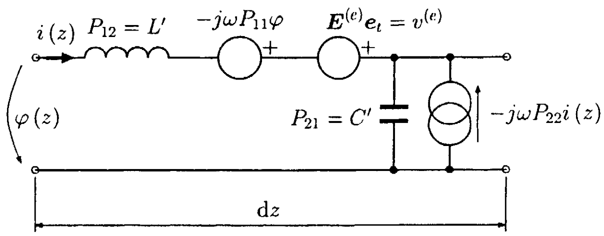

Figure 2: Equivalent circuit for a lossless one-wire structure.

4 Applications and experiments

4.1 Single wire above a ground plane

In the first example a single wire is placed over a perfectly conducting ground plane. (see Fig. 3). The wire is driven by a voltage source and not terminated (open far end) to avoid disturbances from vertical elements. The angle α between the wire and the ground plane is chosen, such that

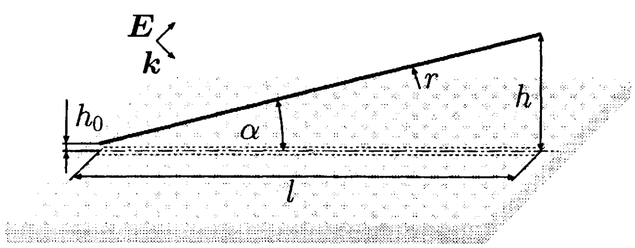

$h_0 = 1$mm
$h = 200$mm
$l = 500$mm
$r = 0.2$mm
$\alpha = 21.7°$
$|\boldsymbol{E}| = 1$V/m

Figure 3: Wire above a perfectly conducting ground plane.

classical transmission-line theory is not applicable any longer. Since the wire is some kind of an antenna it will radiate, and antenna theory or a full-wave method must be used to determine the current through the driving source and the current distribution along the wire. Nonetheless, using classical transmission-line theory and approximating the wire by piecewise uniform line segments yields the result for the input current shown in Figure 4 (a). Additionally, the measured data and the results computed using the full-wave transmission-line theory, but only with the quasi static parameters (0. iteration) are shown. As can be seen there is a significant difference between the piecewise uniform TL and the measurement even for low frequencies.

The resonance frequencies of the transmission-line solution are shifted to higher frequencies, what means that the wire appears electrically shorter than it actually is. Further, the amplitudes at the resonance frequencies are much higher than in the experiment. This is due to the lack of radiation in the transmission-line solution. The solution with FWTLT (quasi static parameters) shows some improvement of the results. For low frequencies there is a very good agreement of the resonance frequencies which means that the electrical length of the wire is correctly taken into account. However, there is still a large deviation of the amplitudes in the resonance regions for higher frequencies, since radiation is not considered.

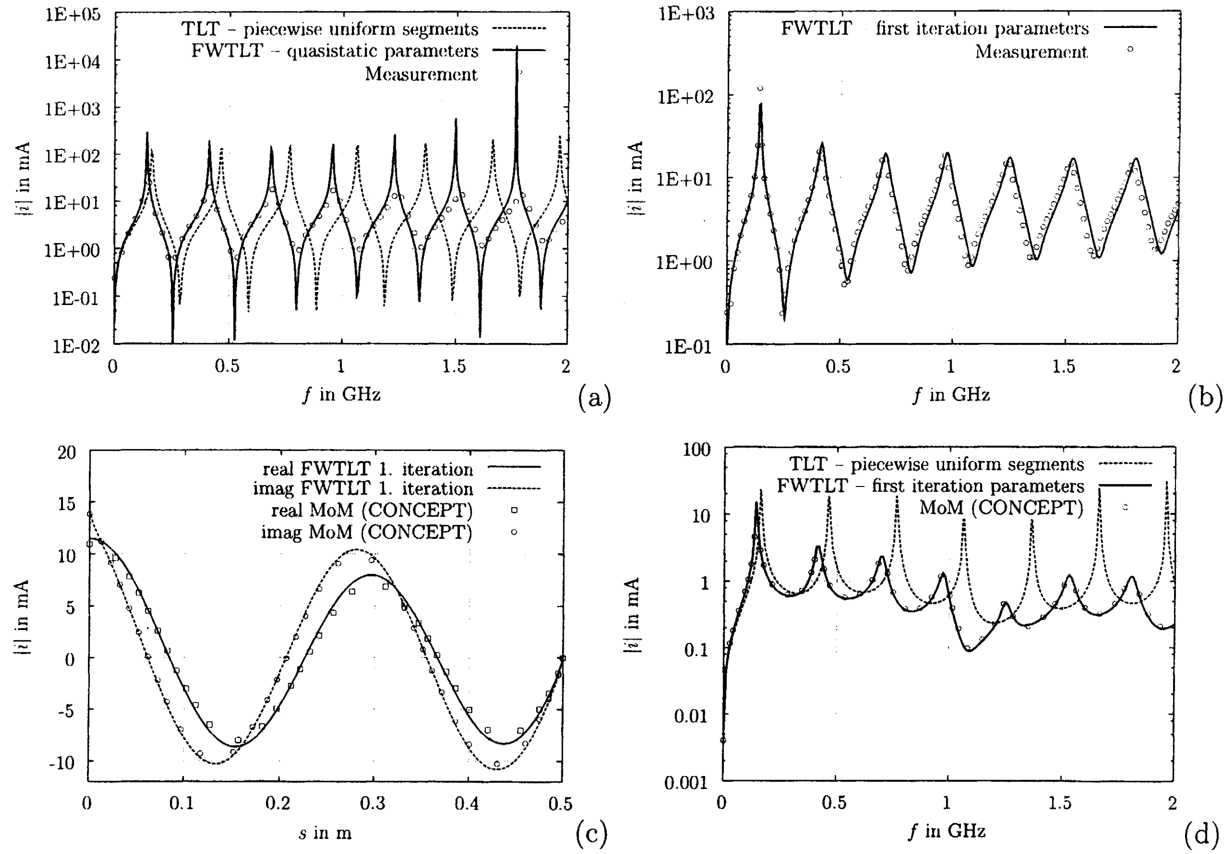

Figure 4: Wire above a perfectly conducting ground plane: Magnitude of the input current of the wire excited by a 1V voltage source, TLT (piecewise uniform segments), FWTLT (quasi static parameters), and measurement (a); FWTLT solutions and measurement (b); Current distribution along the wire at the resonance frequency of 974MHz (c); Magnitude of the input current of the wire excited by a 1V/m plane wave TLT (piecewise uniform segments), FWTLT and MoM solutions (d).

Figure 4 (b) shows the results of the full-wave transmission-line theory with the parameters after the first iteration. Practically, there is no difference between the FWTLT and the measured data. This is supported by the results shown in Figure 4 (c). Here the current distribution determined with MoM and FWTLT along the wire is plotted. The real and imaginary parts of the FWTLT are identical with those from MoM. The wire can also be excited by an external electromagnetic field as shown in Figure 3. For this case the voltage source at the input terminal is removed. Again, the current flowing into the ground plane is considered. Figure 4 (d) shows the results for the FWTLT, the MoM, and TLT (piecewise uniform segments approximation) solutions. Also here the FWTLT and MoM are identical, while the TLT solution shows a significant deviation.

4.2 Crosstalk in a nonuniform multi-conductor transmission line

In the second example crosstalk in a nonuniform multi-conductor transmission line is considered. Figure 5 shows the V-shaped wires which are placed over a ground plane. The angle between the wires is 2α. One wire is at a constant height h, the height of the other wire changes from $h/2$ to h. Furthermore, the wires are bent at the ends in order to reach the termination resistors which are located below the ground plane.

The second wire is driven by a voltage source of 1V with an internal resistance of 50Ω. All other ends are terminated with 50Ω resistors. The electrical connection of the transmission line is shown in Figure 6. Figure 7 shows the cross talk current flowing into the termination resistor at

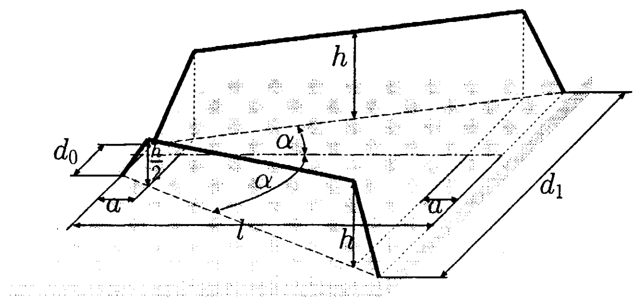

$h = 20\text{mm}$
$d_0 = 16\text{mm}$
$d_1 = 280\text{mm}$
$a = 10\text{mm}$
$l = 435\text{mm}$
$r = 0.2\text{mm}$
$\alpha = 17.7°$

Figure 5: Nonuniform transmission-line configuration.

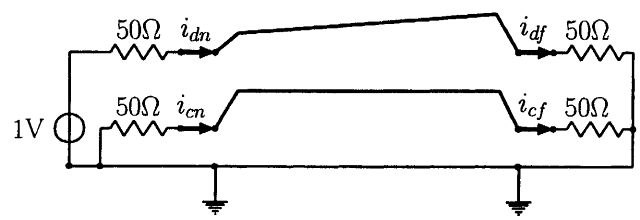

Figure 6: Electrical connection of the nonuniform transmission line.

the far end of the passive wire. The plot presents the solutions from the classical transmission-line theory (with piecewise constant segments) as well as the solution of the full-wave transmission-line theory with the parameters after one iteration. Additionally, the current, measured with a network analyzer on a real setup of the wire structure is shown for validation.

5 Conclusion

The presented full-wave transmission-line theory is a consistent theory based on Maxwell's equations. While the mathematical structure of the primary equations, the telegraphers equations, is preserved, the main difference to the classical TLT are the coefficients (per unit length parameters) which become complex and frequency dependent (even for homogeneous and isotropic surrounding medias). Additionally, new parameters (which are zero in the classical theory) occur, which

360 (12)

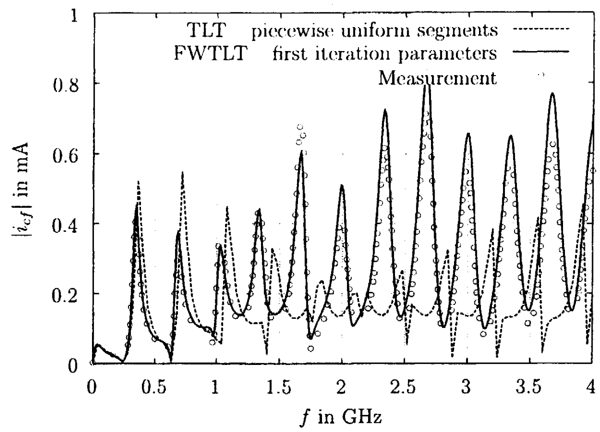

Figure 7: Far end cross talk current of the passive wire of the NMTL.

represent correction terms due to radiation and nonuniformity. These properties have to be taken into account, if high power microwaves couple into complex multiwire structures or ultrawideband excitation is considered.

References

[1] J.B. Nitsch and F. Gronwald, "Analytical solutions in multiconductor transmission line theory," *IEEE Transactions on Electromagnetic Compatibility*, vol. 41, no. 4, pp. 469–479, Nov. 1999.

[2] J. Nitsch, "Exact analytical solution for nonuniform multiconductor transmission lines with the aid of the solution of a corresponding matrix riccati equation," *Electrical Engineering*, vol. 81, pp. 117–120, 1998.

[3] J.B. Nitsch, C.E. Baum, and R.J. Sturm, "Analytical Treatment of Circulant Nonuniform Multiconductor Transmission Lines," *IEEE Transactions on Electromagnetic Compatibility*, vol. 34, 1992.

[4] C.E. Baum, J.B. Nitsch, and R.J. Sturm, "Nonuniform Multiconductor Transmission Lines," Interaction Note 516, Feb. 1996.

[5] F.R. Gantmacher, *The theory of matrices*, vol. 2, New York: Chelsea Publishing Company, 1984.

[6] F.M. Tesche, M.V. Ianoz, and T. Karlsson, *EMC Analysis Methods and Computational Modells*, NY: John Wiley & Sons, Inc., 1997.

[7] C.R. Paul, *Analysis of Multiconductor Transmission Lines*, NY: John Wiley & Sons, Inc, 1994.

[8] R.J. Sturm, "On the Theory of Nonuniform Multiconductor Transmission Lines: an Approach to Irregular Wire Configuration," Interaction Note 541, Jun. 1998.

IGET Institute for
Fundamental Electrical Engineering and Electromagnetic Compatibility

Chair for Electromagnetic Compatibility and Electromagnetic Theory

Univ.Prof. Dr.rer.nat.habil. Jürgen Nitsch

Otto-von-Guericke-University Magdeburg, PF 4120 D–39106 Magdeburg

Dr. Carl E. Baum
AFRL/DEHP Bldg 909
3550 Aberdeen Ave. SE
Kirtland AFB, NM 87117–5776
USA

Dipl.-Ing. Heiko Haase
Institute for Fundamental Electrical Engineering
and Electromagnetic Compatibility

Otto-von-Guericke-University Magdeburg
Universitätsplatz 2
D–39106 Magdeburg
Tel: +49 391 67 11090
Fax: +49 391 67 11236
e-mail: heiko.haase@et.uni-magdeburg.de

Magdeburg, 2000/09/22

Interaction Note

Dear Dr. Baum,

Please find enclosed the revised version of the interaction note proposal. I have incorporated your suggestions and hope everything is ok now.

Yours Sincerly

H. Haase

IN 561

IGET
Institut für
Grundlagen der Elektrotechnik und
Elektromagnetische Verträglichkeit

Lehrstuhl Elektromagnetische Verträglichkeit und Theoretische Elektrotechnik
Univ.-Prof. Dr.rer.nat.habil. Jürgen Nitsch

Otto-von-Guericke-Universität Magdeburg PF 4120 D-39016 Magdeburg

Institut für Grundlagen der Elektrotechnik
und Elektromagnetische Verträglichkeit

Otto-von-Guericke-Universität Magdeburg
Universitätsplatz 2
D-39106 Magdeburg

Tel. +(0391) 67 18 387
Fax. +(0391) 67 11 236
e-mail: juergen.nitsch@et.uni.-magdeburg.de

Dr. Carl E. Baum

Ihre Zeichen, Ihre Nachricht vom	Unsere Zeichen	Hausapparat	Datum
			6. Sept. 2000

Dear Carl:

Enclosed in this letter please find a paper of Haase and myself which we would like to be considered for publication as an Interaction Note.
I think this is a very valuable paper with new important results, in particular in the application field of very high frequencies (HPM, UWB).
We would be very glad, if you can accept it.

Best regards,

Jürgen.